JETIR.ORG ISSN: 2349-5162 | ESTD Year : 2014 | Monthly Issue
JOURNAL OF EMERGING TECHNOLOGIES AND INNOVATIVE RESEARCH (JETIR)
An International Scholarly Open Access, Peer-reviewed, Refereed Journal

EROSIVE WEAR BEHAVIOR OF MICROWAVE PROCESSED WC10Co4Cr CLAD ON SS-316

[1]Paramjit Singh, [2]Dr. Deepak Kumar Goyal, [3*]Dr. Amit Bansal
[1]Ph.D student, [2]Assistant Professor, [3]Assistant professor
[1,2,3] Department of Mechanical Engineering,
[1,2,3] Inder Kumar Gujral Punjab Technical University, Jalandhar, India

Abstract: The current study focused on deposition of protective clad of WC10Co4Cr on alloy steel (SS-316) through microwave technique. The layer was deposited in an industrial microwave oven functioned at 1.20 kW and 2.45 GHz. The XRD observation revealed the cluster of carbide phases in W-Cr-Fe based hexagonal matrix. The SEMsurveillance showed a homogenous reinforced skeleton and dense microstructure with porosity measured less than 1%. The experiment results indicated that Tungsten (W) distributed uniformly in matrix and carbides results bulk hardness. The maximum hardness of the hard protective layer was observed to be 750HV. The erosive wear test performed at different impact angles indicates that the protective clad have significantly less erosive wear than the bare alloy steel (SS-316).

Key words **– hybrid, microwave, heating, clad, hardness, erosive.**

1. INTRODUCTION

Engineering components employed in aerospace, power and petrochemical endure facet deterioration primarily due to erosion. Surface engineering is uttermost extensively used approach for improving the surface properties and functionality of a material without altering its bulk properties [1]. Shield against erosion for ferrous alloys (stainless steel, mild steel) exploited in hydro & thermal power plants is a crucial arena of research. Surface assets of a ferrous alloy could be altering via diverse modes, namely heat treatment, physical vapor deposition (PVD) technique, thermal spurting, epoxy coating, enamel coatings, laser cladding, and microwave cladding [2–7]. Thermal spurting is the most frequently used technique owing to mitigate operation and versatile in nature. Despite that, the frail mechanical bonding amidst splats and the significantly higher porosity are the substantial limitations allied with the thermal spray technique [7–9]. Recently the altering the surface properties of metallic materials using microwave cladding is gaining popularity. At present materials processing induced microwave heating attaining popularity owing to its distinct advantages namely consistent heating, volumetric heating, ameliorate mechanical properties and microstructural characteristics [10-12]. Moreover, microwave processing of the material is also one of the most environmental amiable processes [12]. In microwave processing of materials, the heat generates at the atomic level with in the material which concluded lower energy depletion and increased productivity. In microwaves, the volumetric heat generated with-in the material owing to the atomic level interaction compared to conductive mode of heat transfer in conventional surface heating technique. This phenomenon causes reduced thermal gradient inside the material which leads to curtail remnant stresses with in the material and reformed functional properties [13, 14]. The application of microwave heating in the form of microwave cladding embellish functional properties of metallic material was first clarified by Sharma et al. [15] in a patent form. The authors used microwave heating (MH) technique principles for the evolution of microwave clads exhibit enriched tribological and mechanical properties. The developed clads exhibits the perfect diffusion bonding with the substrate without any interfacial cracking [15]. Afterwards a lot of research executed to ameliorate facet properties of metallic material exploiting economical, low material squander, low power consumption and capacity to produce quality cladding having better tribological performance [16–26].

Alloy steel (SS-316) is one of the uttermost routinely exploit material in many engineering components hold exquisite unification of mechanical concussions such as erosion defiance but is usually perceived as the standard “marine grade stainless steel”, but it is not repellant to warm sea water. The surface properties of SS-316 can be enhanced further by depositing a layer of hard protective layer of WC-10Co-4Cr through hybrid MH. The WC–Co situate materials are preferred by virtue of being superior erosive wear defiance [8–11]. The WC phase offer hardness even though Co phase offer toughness to the overlay material. It has been narrated that the erosive wear resistance of the WC–Co based materials depends on several factors like distribution of the carbide particle size, hardness of the carbide phase and volume fraction of the carbides. The addition of the Cr matrix provides corrosion resistance in oxidizing environment by generating passivating oxide layered structure on the surface of the SS-316, which shields material from foster corrosion and tungsten (W) matrix provides high hardness property leads to low surface erosion of steel substrate [27–29].

The erosive wear of microwave cladded WC10Co4Cr on stainless steel (SS-316) substrate has never been documented.

Microwave cladding can improve the erosive wear resistance of steel alloys such alloy steel (SS-316) by depositing a layer of WC10Co4Cr on its surface. Therefore, in the present work, the surface properties of stainless steel were altered by microwave cladding which is based on the MH technique. Furthermore, several characterization techniques were used to characterize the clad specimens in terms of microstructural, and mechanical (Erosive wear & micro-hardness) performance. The erosive wear behavior of the WC10Co4Cr induced clad specimens was resolute using solid particle erosion in an air jet erosion (AJE) test rig (make: Ducom, model: TR-470) as per ASTM G-76.

2. MATERIALS

2.1 Material details & cladding process

The commercially available WC10Co-4Cr exhibit high hardness and erosive defiance was elected as a clad powder. A typical SEM micrograph evincing the morphology of the WC10CO-4Cr powder is shown in figure 2.1. The shape of the powder is mainly spherical with a size distribution of 40 ± 5 µm diameter. The alloy steel (SS-316) specimens of size (20 x 20 x 5 mm) was taken as a base material. The chemical compositions (wt. %) of the substrate (SS-316) and WC-10CO-4Cr powder as obtained by the optical emission spectrometer (OEM) are given in Table 2.1.

Table 2.1 The elemental composition (wt %) of the material used for development of cladding.

Element Composition (wt%)	Cr	Co	Mn	W	Ni	Mn	C	Fe	Mo	Si
SS-316	17.8	--	2.1	--	13.8	2.1	0.08	72	2.9	0.023
WC10Co4Cr	4.28	11.62	---	65.67	---	----	8.43	---	---	-----

The preparation of clad powder and substrate is essential for clad development. Prior to clad deposition, the SS-316 substrate was ultrasonically cleaned in an ethanol bath. To remove any possible moisture, the WC10CO4Cr clad powders were warmed in a muffle furnace at 120°C for 8 hours. The clad powder was manually applied to the substrate, with an average thickness of around 1 mm. A multimode industrial microwave oven was used to melt the preplaced clad powder on the SS-316 substrate [15-26]. The clad powders were uniformly propagated on the substrate upper surface, with an average thickness of about 1 mm. On the preplaced powder, an alumina plate (separator) with a thickness of about 0.5 mm was preserved, and expedite susceptor powder (charcoal) was placed on the alumina plate. Following that, the entire assembly was placed in the microwave oven cavity and subjected to electromagnetic microwave radiation. Through a series of trial runs, the optimal process parameters were determined. Figure 2.2 shows a schematic of the experimental equipment used to deposit the protective hard layer using a microwave approach. Hybrid MH principles were successfully applied to the deposition of protective hard layer on the substrate surface. The susceptor powders (charcoal) have a high loss tangent easily absorb microwave energy at room temperature. After heated to high temperature, the susceptor transferred heat to the clad powder through the alumina plate (separator) via conduction mode of heat transfer. The temperature of the clad powder begins to rise until it reaches the threshold temperature, at which point the powder particles themselves begin to mesmerize microwave radiation, causing the clad powder to melt.

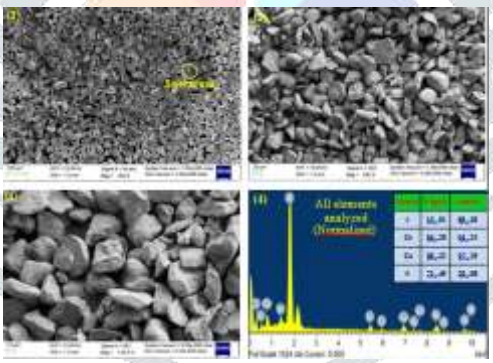

Fig. 2.1 Typical SEM & EDS micrograph of WC10CO4Cr powder particles

Table 2.2 Microwave processing parameters utilized for WC10CO4Cr clad development.

Parameters	Values	Units
Powder	40 ±5	µm
Powder pre heat temperature	120	°C
Microwave power	1.2	KW
Frequency	2.45	GHz
Time of exposure	600	Sec.
Processing environment	Ambient	

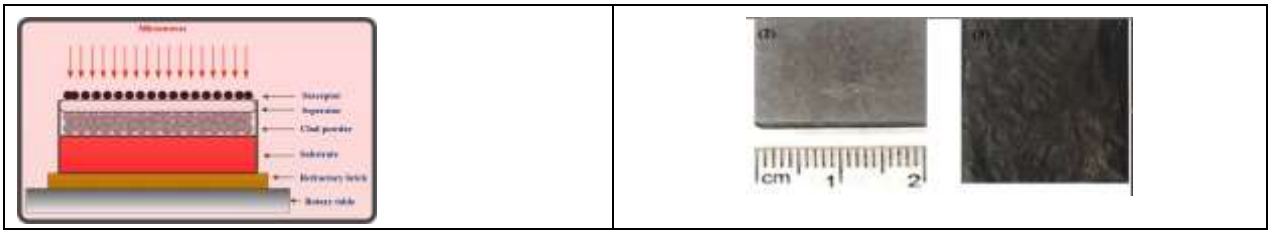

Fig. 2.2 Schematic: (1) Microwave oven cavity (2) specimen size (3) cladded steel surface.

3. CHARACTERIZATION TECHNIQUES

A WC10CO4Cr cladded specimen was cold mounted in epoxy after being sliced across the thickness with a low speed diamond saw (make: Chennai Metco, model: BAINCUT LSS). The mounted specimens were ground and polished down to 2000 grit with emery sheets, then polished with 1 mm diamond paste on the canvas. A Carl Ziess SEM (model: Gemini Ultra Plus) was used to do microstructural characterization on the WC10CO4Cr clads. The partial dilution of clad powder and steel substrate particles on steel surface was assessed using a Carl Ziess SEM (model: Gemini Ultra Plus) equipped with an image analysis software tool (Dewinter Material Plus, Version 5.2). To assess microstructural characteristics, back- scattered electron (BSE) micrographs along the polished cross-sectional surfaces were taken. At 50 g load and 10 s dwell time, the micro hardness of the WC10CO4Cr clads was evaluated using a Vickers' micro hardness tester (make: Chennai Metco, model: Economet VH1 MD). Starting from the acme of the clad and working towards the substrate, indentations were made with every 100 µm.

3.1 Erosive wear test

The WC10Co4Cr microwave clads erosive wear behaviour was assessed by utilizing a solid particle erosion in an air jet erosion (AJE) test apparatus (make: Ducom, model: TR-470) according to ASTM G -76, as illustrated in figure 3.1. The inset SEM micro images exemplify erratic shaped morphology of the alumina particles as shown in figure 3.2.

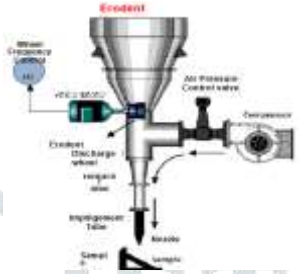

Fig. 3.1 Schematic Air jet erosion test rig

The alumina particles had a roundness value of 0.40, which was determined. Alumina is utilised as an abrasive because of its extreme hardness and trigonal bravais lattice or hexagonal closed packed structure.

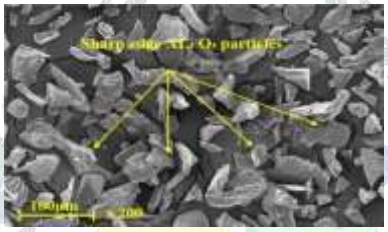

Fig. 3.2 Pure Alumina (Al_2O_3) powder in a distinct BSE picture

The erodent powder was loaded into the hopper and then fed into the air line via a spinning grooved disc that controlled the erodent feed rate. The air-erodent combination was forced out at high velocity with a tungsten carbide (WC) nozzle with a 1.5 mm diameter. A revolving double disc configuration offered in the AJE test rig was used to monitor the erodent jet velocity. Three specimens were tested for 30 minutes, with the weight change being measured every 2 minutes. The AJE test apparatus was allowed to reach a steady condition; hence data on weight loss after the first 2 minutes was assessed. The erosive wear test was carried out at three different impact angles (30°, 60°, and 90°), as shown in figure 3.3. The erosive test parameters will be showed in in Table 3.1. The specimens were weighed before and after being ultrasonicated in acetone. The mean value of weight loss of these two specimens at each impact angle scenario i.e. un-cladded and WC10CO4Cr cladded was also utilized to compute cumulative weight loss and erosion rate in terms of weight loss per unit erosion time (mg/min). Further, the erosion coefficient (ε) was determined and given as the ratio of volume loss from the specimen to erodent discharge rate.

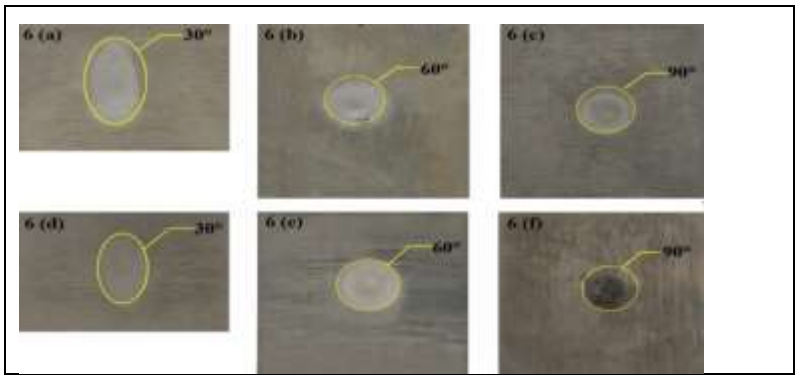

Fig. 3.3 Austenitic stainless steel specimens after conducting erosive wear test at an impingement angles of (30°, 60° and 90°)

Table: 3.1 Erosive wear test parameters:

Testing Parameters	Value	Units
Scheme	Air jet erosion	-
Erodent	Alumina	-
Erodent hardness	1800-2000	HV
Erodent particle size	50±5	µm
Erodent feed rate	2.5±1	g/min
Erodent velocity	50±3	m/s
Specimen size	22 x 22 x 5	mm
Specimen to nozzle distance	10	mm
Impact angle	30 , 60 , 90	deg
Total erosion time	30	min
Ambient testing temperature	27±3	°C

3. RESULTS AND DISCUSSION

3.1 Microstructural Analysis:

The clad's microstructure has a big impact on its tribological properties. The microwave- induced clad, which is around 1 mm thick, shows excellent metallurgical bonding with substrate. Typical back scattered electron (BSE) cross-sectional micrograph images as shown in figure 3.1 were studied using SEM to assess microstructural characterization. The tungsten carbide (W_2C) and free tungsten would clearly have identified that cladding is free from interfacial cracks and visible porosity. Alloying elements present in substrate and WC10CO4Cr powder particles were uniformly distributed along clad region i.e. complete partial dilution of substrate and clad elements is an indication of uniform heating. It is observed that possible decomposition of WC form starting powder into free W & W_2C at high temperature during microwave heating as represented in Eq. 2 & 3.

$WC \rightarrow W+C$ ---------- (2)

$WC+W \rightarrow W_2C$---------- (3)

This free carbon might react with atmospheric oxygen to form CO which escapes subsequently during solidification leads to crack free clad and less porosity. Residual free carbon further reacts with binder cobalt and free tungsten (W) to form complex carbides. Metallic carbides are formed when highly reactive free carbon combines with powder and substrate like Co2, Cr_2C_6, $CO_3W_9C_4$ represented in Eq. 4 & 5.

$9W+3Co+4C \rightarrow Co_3W_9C_4$ ---------- (4)

$6Fe+6W+C \rightarrow Fe_6W_6C$ ---------- (5)

Further thermal gradient leads to heat transfer which is weak due to volumetric heating. co- efficient of both substrate and clad material. Microstructure of WC10CO4Cr cladded specimen observed like those of reinforced composite with a domination skeleton structure as shown in figure 6 (4 & 5) i.e. augmentation of binary carbides of W & Fe in metallic matrix.

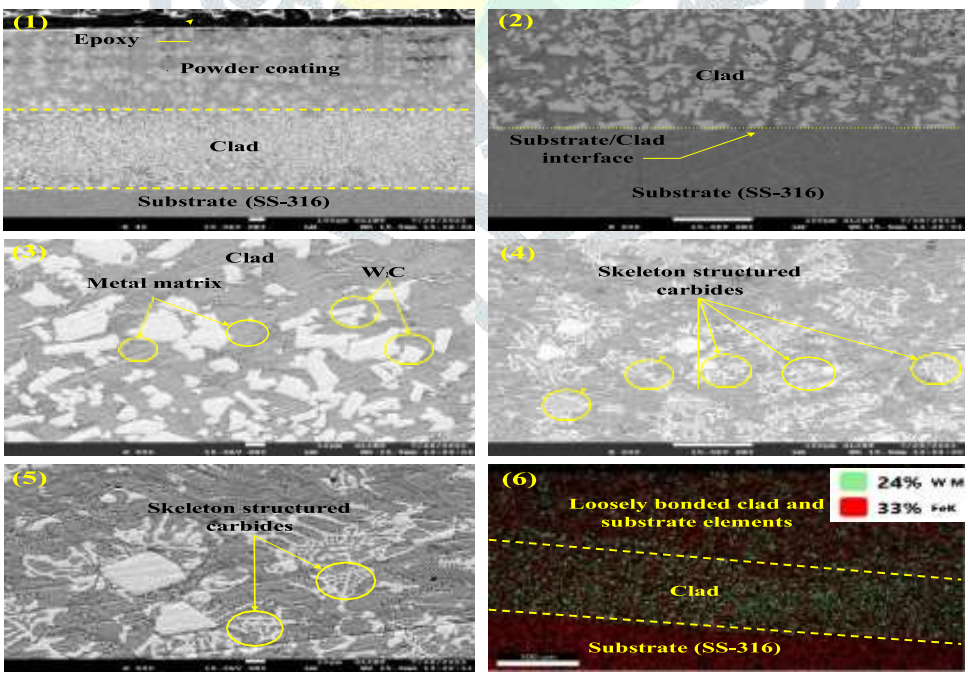

Fig. 3.1 Typical BSE images across sectional thickness of WC10CO4Cr Cladded specimen

1. 2 Erosive wear analysis

The cumulative weight loss and erosion rate in terms of weight loss per unit erosion time (mg/min.) were calculated using the mean value of weight loss of these two specimens i.e. un-cladded and WC10CO4Cr cladded, as shown in observation table no. 3.1. As stated in table no. 3.2, the erosion coefficient (ε) was determined and given as the ratio of volume loss from the specimen

to erodent discharge rate. At a 30° impingement angle, weight loss (0.052) in plain SS-316 is clearly more than weight loss (0.002) in WC10CO4Cr cladded specimens. Less erosion is caused by the wear resistance and high hardness of the WC10C04Cr cladded surface. The magnitude of the erosion coefficient, determined from cumulative weight loss, is $8.6775x10^{-3}$, which is likewise higher at a 30° impingement angle in an unclad steel specimen, as shown in figure 3.2. It is very clear from the figure 3.2 (1) at an impingement angle of 30°abrassion, ploughing and micro cutting between clad and substrate particles are more in comparison to WC10CO4Cr cladded specimen as shown in figure 3.2 (4). Particle impacts within the incident stream, a wide range of simultaneous attack angles, particle fragmentation, carbide pull-outs, embedded particle lip formation, micro-cutting of matrix and cladding, severe abrasion between clad and erodent particles, surface shielding due to rebounding particles, and particle embedding effects are just a few of them. (Some of these effects, such as fragmentation and embedding, can also occur when a single particle collides with another.) Subsurface damage as a result of many strikes is another key effect.

Table: 3.1 Cumulative weight loss observations.

Material	Impact angle (deg)	Weight (gm's.) change/loss after 05 minutes								
		Initial weight	5min	10min	15min	20min	25min	30min	Final weight	Weight loss
SS-316	30	19.183	19.148	19.130	19.149	19.134	19.131	19.131	19.131	**0.052**
	60	24.495	24.502	24.503	24.497	24.494	24.493	24.493	24.493	**0.002**
	90	24.134	24.135	24.134	24.128	24.133	24.132	24.132	24.132	**0.002**
SS-316 (WC10CO4Cr cladded)	30	17.475	17.477	17.475	17.473	17.474	17.473	17.473	17.473	**0.002**
	60	21.359	21.361	21.350	21.359	21.358	21.357	21.357	21.357	**0.002**
	90	21.535	21.537	21.536	21.535	21.534	21.533	21.533	21.533	**0.002**

Table: 3.2 Calculation for cumulative weight loss and average erosion value.

Calculation's for measuring Average erosion value								
Material	Impact angle (deg)	Initial wt. (mg.)	Final wt. (mg.)	Weight loss (mg.)	Volume loss =Wt. loss / Density of specimen material	Volume loss	Erodent consumed =Feed rate x time Erodent consumed =2.5x30	Avg. erosion value (mm^3/gm)
SS-316	30	0.019183	0.019131	0.000052	0.000052 / 0.00799	0.006508135	75 gm	8.67751 x $\mathbf{10^{-3}}$
	60	0.024495	0.024493	0.000002	0.000002 / 0.00799	0.00025 0313	75 gm	3.33751 x $\mathbf{10^{-6}}$
	90	0.024134	0.024132	0.000002	0.000002 / 0.00799	0.00025 0313	75 gm	3.33751 x$\mathbf{10^{-6}}$
Clad specimens	30	0.017475	0.017473	0.000002	0.000002 / 0.00799	0.00025 0313	75 gm	3.33751 x $\mathbf{10^{-6}}$
	60	0.021359	0.021357	0.000002	0.000002 / 0.00799	0.00025 0313	75 gm	3.33751 x $\mathbf{10^{-6}}$
	90	0.021535	0.021533	0.000002	0.000002 / 0.00799	0.00025 0313	75 gm	3.33751 x $\mathbf{10^{-6}}$

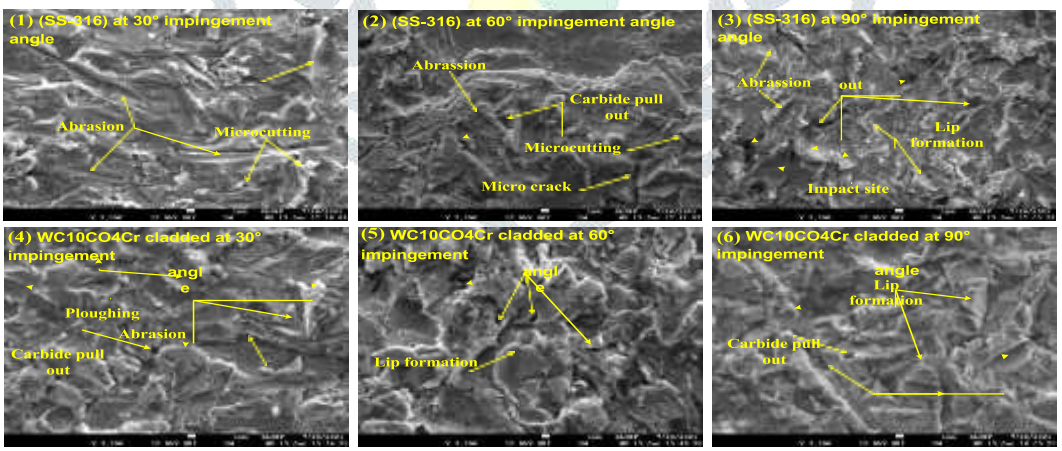

Fig. 3.2 BSE images area impression on plain SS-316 & WC10CO4Cr Cladded specimen

3.3 Microhardness study

A Vickers's micro hardness tester (make: Chennai Metco, model: Economet VH1 MD) was employed to evaluate the micro hardness of un-cladded and WC10CO4Cr cladded specimen at 50 g load, 0,025Kgf force and 10 second dwell time. The micro image of indents and micro-hardness value of an austenitic stainless steel (SS-316) ranges from 300–450 HRV as shown in figure 3.3. Figure 3.4 illustrate indentations made at 100µ m intervals starting from the top of the substrate and progressing to the clad.

Fig. 3.3 Micro images of indents from plain austenitic stainless steel (SS-316)

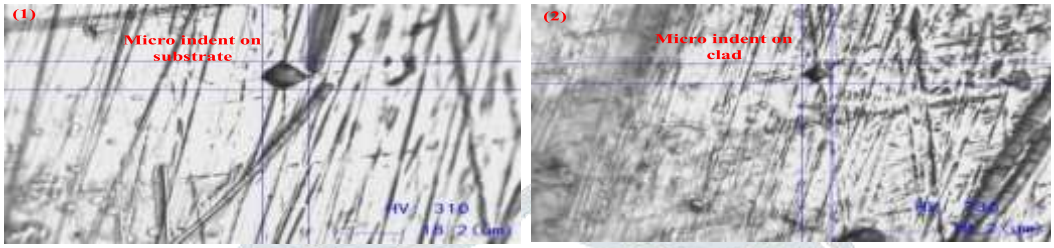

Fig. 3.4 Micro images of indents from substrate to WC10CO4Cr clad region

It is clearly observed from figure 3.4 that Vicker's hardness indents appeared from substrate to clad region. Numbers of indents so produced from substrate to clad has variation in their size and shape i.e. more the indent size lesser the hardness value and vice versa. Micro indent size refer figure 3.4 (1) differ from indent size refer figure 3.4 (2). Less value of micro hardness is due to the metallic matrix of tough metals like (Co & Fe). As we measured micro hardness from substrate region to clad region at an interval of 100 µm sizes of indents changes from large to small is an indication of hardness variation and corresponding values of hardness can assessed. Micro hardness of WC10CO4Cr cladded region in more than the substrate SS-316 region because of uniform distributed particles of substrate and clad as depicts in figure 3.4 (1 & 2). Presence of metallic carbides, no intermetallic cracks, better partial dilution of clad and substrate can lead to more micro hardness ranges from 400-750 HV in comparison with micro hardness of austenitic stainless steel (SS-316) un-cladded specimen clearly seen as shown in figure 3.5

Fig. 3.5 Plain (SS-316) vs. WC10CO4Cr clad specimen hardness comparison

4. Conclusion

Microwave cladding has been proven as a unique processing approach for developing cladding on metallic substrates. A schematic model has been used to describe the mechanics of clad generation. WC10Co4Cr cladding on austenitic stainless steel (SS-316) was produced in this study, and microstructural characterization, erosive wear behavior, and electrochemical corrosion tests were performed. The following are some of the work's major conclusions:

- Metal-based clads on metal-based substrates can be successfully developed using hybrid MH technique.
- By partial mutual diffusion of elements and grain growth extending from the diluted substrate towards the formed clad, the developed clad is metallurgical bonded to the austenitic stainless steel substrate.
- The developed clad microstructure has skeleton structured carbides and free from intermetallic cracks morphology with no transition of cell to dendrites.
- Nickel is homogeneously segregated inside the cells, while chromium and tungsten (in the form of carbides) are segregated at cell boundaries. Around the cell borders, the segregated chromium and tungsten interacts with carbon, forming metallic carbides.
- The developed clad exhibit good erosive wear resistance property owing to the high hardness due to presence of metallic carbides i.e. WC &W_2C, Cr_2C_6 etc.
- Average erosion value of austenitic stainless steel (SS-316) substrate was approximately 61% more than WC10Co4Cr cladded steel substrate. R

Acknowledgment:

The author would like to evince gratefulness to Science and Engineering Research Board (SERB), India for financing this work with project no. SRG/2019/001182.

REFERENCES

[1] Thostenson, E.T. and Chou, T.W., 1999. Microwave processing: fundamentals and applications. *Composites: Part A*, 30, pp.1055–1071

[2] Sutton, W.H., 1989. Microwave processing of ceramic materials. *American Ceramic Society Bull*, 68(2), pp. 376–86.

[3] Das, S., Mukhopadhyay, A.K., Datta, S., Das, G.C. and Basu, D., 2007. Prospectus of microwave processing: An overview. *Material science*, 32, pp. 1-13.

[4] Sharma, A.K., Mishra, R. R., 2017. Role of particle size in microwave processing of metallic material systems, *Journal of Materials Science and Technology*, 34(2), pp. 123-137.

[5] Dheeraj, G. and Sharma, A.K., 2011. Development and microstructural characterization of microwave cladding on austenitic stainless steel. *Surface & Coatings Technology* 205, pp.5147–5155.

[6] Dheeraj, G. and Sharma, A.K., 2011. Microstructural characterization of cermet cladding developed through microwave irradiation. *Journal of Materials Engineering and Performance.* 21, pp.2165-2172.

[7] Zafar, S. and Sharma A.K., 2014. On friction and war behaviour of WC-12Co microwave clad, *Tribology Transactions*, 28, pp. 584–591,

[8] Kaushal, S., Sirohi, V., Gupta, Dheeraj., Bhowmick, H. and Singh, S., 2015. Processing and characterization of composite cladding through microwave heating on martensitic steel, *Proc I MechE Part L: J* Materials: *Design and Applications* 232, pp80-86.

[9] Zafar, S. and Sharma, A.K., 2016. Abrasive and erosive wear behaviour of nano metric WC–12Co microwave clads. Wear 346-347, pp. 29-45.

[10] Zafar, S. and Sharma, A.K., 2016. Prediction of tribological behaviour of WC-12CO nanostructured microwave clad through ANN , *Tribology Online*,11, pp. 333-340.

[11] Gaonkar, A., Hebbale, A.M. and Srinath, S.M., 2016. Microwave cladding and characterization of WC-12Co on nickel based superalloy, *IJERMCE*, pp. 2456-1290

[12] Vasudev, H., Singh, G., Bansal, A. and Vardhan, S., 2019. Microwave heating and its applications in surface engineering: a review. Mater. Res. Express, 6, pp. 102001.

[13] Kaushal, S., Gupta D. and Bhowmick, H., 2016. On microstructure and wear behaviour of microwave processed composite clad, *Journal of Tribology*. 139, pp. 061602-061608.

[14] Zafar S., Bansal A., Sharma A.K., Arora N. and Ramesh C.S., 2014. Dry erosion wear performance of Inconel 718 microwave clad, *Surface Engineering*, 30, pp. 852-85

[15] Hebbale, A.M. and Srinath, M.S., 2017. Taguchi analysis on erosive wear behaviour of cobalt based microwave cladding on stainless steel AISI-420, *Measurement*, 99, pp. 98-107.

[16] Goldstein K.J. and Yakowitz, H., 1975. Practical scanning electron microscopy: *Electron and ion microprobe analysis* , New York- Plenum Press, pp. 582.

[17] Akshata, M.K., Hebbale, A.M. and Srinath, M.S, 2018. Sliding wear studies of microwave clad versus unclad surface of stainless steel 304. *MATEC Web Conf*., 144, 02010.

[18] Clark, D.E., Folz D.C. and West, J.K., 2000, Processing materials with microwave energy, *Mater. Sci. Engg.*, 287, pp. 153–158.

[19] Kaushal, S., Singh, D., Gupta, D., Bhowmick, H. and Jain, V. 2018. Processing of Ni20WC10Mo based composite clads on austenitic stainless steel through microwave hybrid heating, *Materials Research Express*-5, 036401.

[20] Das,S., Mukhopadhya M.K., Datta S., Das G.C. and Basu, D., 2008. Prospects of microwave processing: An overview**,** *Bulletin of Materials Science*, 31, pp. 943–956.

[21] Mishra, R.R. and Sharma, A.K., 2016. Microwave-material interaction phenomena: heating mechanisms, challenges and opportunities in material processing. *Composites: Part A: Applied Science and MAnufacturing*, 81, pp. 78-97.

[22] Kaushal, S., Singh, D., Gupta, D., and Jain, V. 2019. Processing of Ni-WC-Cr3C2- based metal matrix composite cladding on SS-316L substrate through microwave irradiation. *Journal of Composite Materials*, 53(8), 1023-1032.

[23] Kaushal, S., Singh, D., Gupta, D., and Jain, V. 2019. Wear resistance improvement of austenitic 316L steel by microwave processed composite clads. Journal of Tribology, 141(4), 041605.

[24] Singh, B., Kaushal, S., Gupta, D., and Bhowmick, H.L. 2018. An development and dry sliding wear behavior of microwave processed Ni/Al_2O_3 composite clad, *Journal of Tribology*, 140(6), 061603

[25] Kaushal, S., Gupta, D., and Bhowmick, H.L. 2018. On development and wear behavior of microwave-processed functionally graded clads on SS-304 substrate, *Journal of Materials Engineering and Performance*, 27(2), 777-786.

[26] Kaushal, S., Gupta, D., and Bhowmick, H.L. 2018. Investigation of dry sliding wear behavior of Ni-SiC microwave cladding, *Journal of Tribology*, 139(4), 041603.

[27] Sutton, W.H., 1992. Microwave processing of ceramics—an overview, In: Beatty RL, Iskander MF, Sutton WH, editors. Microwave processing of materials III, *Materials Research Society Proceedings. Pittsburgh: Materials Research Society*, pp2-3.

[28] Bansal, A., Sharma, A.K., Kumar, P. and Das, S., 2014. Investigation on microstructure and mechanical properties of the dissimilar weld between mild steel and stainless steel-316 formed using microwave energy. *Proc Inst Mech Eng B J Eng Manuf* . 230, pp. 439-448.

[29] Mago, J., Bansal, S., Gupta, D. and Jain, V., 2020. Influence of microwave heating on metallurgical and mechanical properties of Ni-40Cr_3C_2 composite clads in the context of cavitation erosion resistance characteristics, *Metallurgical and Materials Transactions,* 51, pp. 4288–4300